

Available at [www.sciencedirect.com](http://www.sciencedirect.com)

ScienceDirect

journal homepage: [www.elsevier.com/locate/carbon](http://www.elsevier.com/locate/carbon)

# Analysis of carbon nanotube shortening and composite strengthening in carbon nanotube/aluminum composites fabricated by multi-pass friction stir processing

Z.Y. Liu <sup>a</sup>, B.L. Xiao <sup>a</sup>, W.G. Wang <sup>b</sup>, Z.Y. Ma <sup>a,\*</sup>

<sup>a</sup> Shenyang National Laboratory for Materials Science, Institute of Metal Research, Chinese Academy of Sciences, 72 Wenhua Road, Shenyang 110016, China

<sup>b</sup> Liaoning Shihua University, 1 Dandong Road, Fushun 113001, China

## ARTICLE INFO

### Article history:

Received 24 July 2013

Accepted 9 December 2013

Available online 12 December 2013

## ABSTRACT

Carbon nanotubes (CNTs) were dispersed into Al matrix by multi-pass friction stir processing (FSP) to fabricate 4.5 vol.% CNT/2009Al composites. The maximum strength of the composites was obtained with three-pass FSP and was attributed to the combined effect of CNT cluster reduction, grain refinement, and CNT shortening. A CNT shortening model is proposed to describe the CNT length change with FSP passes. The model indicates that the reciprocal of the CNT length has a linear relationship with the duration of the mechanical effect, which was verified by our and other investigators' experimental results on various mechanical processes. Based on the concept of the load transfer efficiency of CNTs in the Al matrix, a universal strength model considering the microstructural parameters – the aspect ratio of CNTs, grain size, and concentration of CNT clusters and pores – is proposed to predict the strengthening of the CNT/2009Al composites with and without CNT clusters. The predictions are in good agreement with the experimental results.

© 2013 Elsevier Ltd. All rights reserved.

## 1. Introduction

With extremely high strength (>30 GPa) and modulus (about 1 TPa) as well as low density and good physical properties [1–5], carbon nanotubes (CNTs) are considered to be an ideal reinforcement for metal matrix. However, it is very difficult to disperse the CNTs in the metal matrix, not only because of the entanglement or bundling of the CNT clusters as a result of their large aspect ratio and strong van der Waals' force, but also due to poor compatibility of the properties of CNTs and metals [6–9].

In the past few years, many fabrication methods, for example casting [10], spraying [11,12], powder metallurgy

(PM), and molecular level mixing [13], have been tried to disperse CNTs into the metal matrix. Among the reported methods, the casting process encounters the problems related to poor wetting and chemical reaction between the CNTs and metal melt. The plasma spraying processing can easily produce CNT-Al powders, but CNT clusters appear at high CNT concentration. The molecular-level mixing method can disperse CNTs uniformly but it is hard to use this method to fabricate CNT-reinforced Al composites. The PM route has been commonly used to fabricate CNT/metal composites [14–16] because it makes it easier to incorporate the CNTs into the metal matrix. Ball milling is a commonly used technology for dispersing reinforcement in the PM route.

\* Corresponding author. Fax: +86 24 83978908.

E-mail address: [zyrna@imr.ac.cn](mailto:zyrna@imr.ac.cn) (Z.Y. Ma).

0008-6223/\$ - see front matter © 2013 Elsevier Ltd. All rights reserved.

<http://dx.doi.org/10.1016/j.carbon.2013.12.025>

Ball milling can disperse nano-sized particles into the metal matrix due to its repeated deformation, cold-welding, and fracture processes [17]. Recently, ball milling was widely used to fabricate CNT/metal composite powders [18–20]. Although the ball-milling process is one of the most promising routes for preparing CNT/metal composites, it would contaminate the composite powders and cause severe damage to the CNTs because of its large energy input as well as the lengthy treatment time.

Friction stir processing (FSP), a development based on the basic principles of friction stir welding, is a relatively new metal-working technique. A schematic of FSP is shown in Fig. 1. During FSP, the rotating threaded pin imposes severe plastic deformation and material mixing, thereby uniformly distributing the CNTs into the metal matrix [21]. Johannes et al. [22] and Morisada et al. [23] fabricated CNT/aluminum alloy and magnesium alloy surface composites, respectively, by inserting the CNTs into the holes or grooves pre-machined on the alloy plates and then subjecting the plates to FSP. They found that a good CNT dispersion was achieved after FSP.

In our previous study [24], a new route was established to fabricate the CNT/Al composites by combining the PM technique with four-pass FSP, where the composite billet with clustered CNTs fabricated by PM was subjected to FSP to disperse the CNTs. It was shown that the FSP CNT/2009Al composites exhibited a uniform dispersion of CNTs and considerably improved yield strength (YS).

Although increasing the number of FSP passes could improve the CNT distribution in the composites, extended mechanical processing would shorten the CNTs significantly, and this reduces the efficiency of load transfer from the metal matrix to the CNTs, which was considered as one of two strengthening mechanisms for the CNT/Al composites [24]. Thus, predicting and controlling the CNT length variation during FSP or other mechanical processes is of critical importance.

Grain refinement was commonly reported in FSP aluminum and magnesium alloys. In CNT/Al composites, the grain refinement, which is another strengthening mechanism, was related to the dispersed CNTs [24]. As the number of FSP passes increased, the grains of the CNT/Al composites could be further refined because more CNTs were uniformly

dispersed into the Al matrix. CNT shortening and grain refinement affect the composite strength in opposite ways. A quantitative strengthening model is needed to describe these complicated influences.

In our previous study [24], a strength model has been proposed, considering the load transfer and grain refinement, to predict the strengthening of the CNT/Al composites, and the model prediction was in good agreement with the experimental results of the composites with individually dispersed CNTs. However, the CNT clusters and resultant pores, which were common problems in the CNT/Al composites fabricated using various routes, were not considered. In this case, it is important to establish a universal strength model to describe the strengthening of the CNT/Al composites with or without the CNT clusters.

In this study, 4.5 vol.% CNT/2009Al composites were fabricated by a combination of PM and multi-pass FSP. The shortening of the CNT length during FSP was analyzed based on the microstructural observations and linearized Weibull model. The relationships between the microstructural parameters, that is, the aspect ratio of CNTs, grain size, porosity ratio, and the YS of the composites, were discussed. The aims are (a) to optimize the FSP passes to obtain the best mechanical properties of the composites, (b) to propose a model to predict the CNT shortening during mechanical processing, and (c) to establish a universal model to describe the strengthening of the CNT/Al composites with or without the CNT clusters.

## 2. Experimental

### 2.1. Raw materials and composite fabrication

As-received CNTs (Fig. 2(a)) with an outer diameter of 10–20 nm and a length of  $\sim 5 \mu\text{m}$  were mixed with 2009Al powders, with an average diameter of  $10 \mu\text{m}$  (Fig. 2(b)), in a bi-axis rotary mixer at 60 rpm for 8 h with a 1:1 ball to powder ratio. The volume fraction of CNTs in the mixed powders was 4.5%. The as-mixed powders were cold-compacted in a cylinder die, degassed, and then vacuum hot-pressed into cylindrical billets, with a diameter of 55 mm and a height of 50 mm, at 833 K for 1 h.

The as-pressed billets were then hot forged at 723 K into disc plates with a thickness of about 10 mm. Then the plates were subjected to in situ one- to five-pass FSP at a tool rotation rate of 1200 rpm and a travel speed of 100 mm/min, using a tool with a concave shoulder 20 mm in diameter and a threaded cylindrical pin 6 mm in diameter and 4.2 mm in length. The penetration depth of the pin was 4.5 mm. For comparison, unreinforced 2009Al was also fabricated under the same conditions. The as-FSP composites and the 2009Al alloy were solutionized at 768 K for 2 h, water quenched, and then naturally aged at room temperature for 96 h. The aged composites were used for microstructure observation and tensile testing.

### 2.2. Characterization of the composites

The CNT distribution in the matrix under various fabrication conditions was examined using scanning electron microscopy

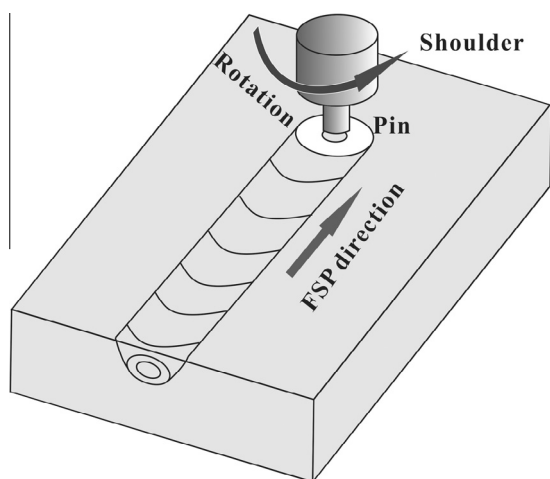


Fig. 1 – Schematic of friction stir processing.

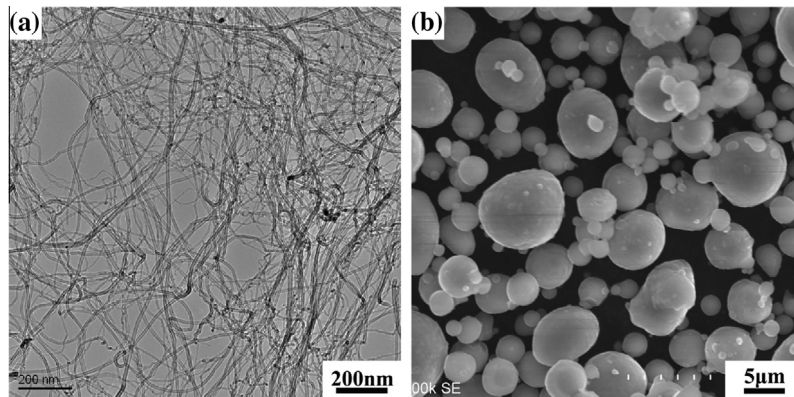


Fig. 2 – Morphologies of as-received (a) CNTs and (b) 2009Al powders.

(SEM, Quanta 600), field emission scanning electron microscopy (Leo Supra), and transmission electron microscopy (TEM, Tecnai G2 20). CNT clustering fractions were analyzed using image analysis software (Image-Pro Plus 6.0). The CNTs were extracted from the as-FSP composites by corroding the aluminum matrix using dilute hydrochloric acid and followed by using dilute ferric chloride aqueous solution. Then the residues were rinsed with water and filtered. To avoid re-aggregation of the CNTs, the extracted CNTs were dispersed in 1.5 wt.% sodium dodecylbenzene sulfonate aqueous solution. The dispersed solution was dropped on a Cu net coated with carbon member. The Cu net was washed by dropping acetone and then dried for TEM observation to estimate the CNT length and diameter. At least 80 CNTs were counted. The densities of the composites were determined using the Archimedeian principle, with distilled water as the liquid for the measurement. At least three samples were tested to obtain accurate average values.

Tensile specimens with a gauge length of 2.5 mm, a width of 1.5 mm, and a thickness of 0.9 mm were electro-discharge machined from the FSP composites perpendicular to the FSP direction and polished using abrasive papers of meshes 800 and 2000. Tensile tests were conducted at a strain rate of  $1 \times 10^{-3} \text{ s}^{-1}$  at room temperature using an Instron 5848 Microtester. For comparison, the tensile tests of the 2009Al and the as-forged composites were conducted under the same conditions.

### 3. Results

#### 3.1. Microstructure of the composites

Fig. 3 shows the CNT distribution in the forged and FSP composites. Obvious CNT clusters, aligned along the flow direction of the forging, with sizes from 1 to  $6 \mu\text{m}$  could be observed in the forged composite. Almost no aluminum was found to be immersed in the clusters, mainly due to the nano-sized pores and poor wetting property between CNT and the aluminum matrix. By comparison, only a small number of small CNT clusters were detected in the one-pass and two-pass FSP composites. In the three-pass FSP composite, almost no CNT clusters could be found. This is similar to the result reported by Morisada et al. [23], who also found that one-pass FSP was insufficient to completely eliminate CNT

clustering. As the number of FSP passes increased to three to five, even the small clusters could not be found using SEM. This implies that the uniformity of the CNT distribution could be greatly improved by increasing the number of FSP passes.

Fig. 4 shows the morphology of the CNTs extracted from various FSP composites. Two observations could be made. Firstly, no obvious diameter change was observed as the number of FSP passes increased from one to five. The average diameter of CNTs gradually changed from 11.8 to 10.6 nm as the FSP pass increased from one to five, which implied that the tube structure of the CNTs did not suffer severe damage during FSP. Secondly, the length of the CNTs decreased continuously as the number of FSP passes increased from one to five due to accumulated damage to the CNTs caused by multiple-pass FSP. In the five-pass FSP composite, the average CNT length decreased to about 250 nm.

Fig. 5 shows the CNT distribution and the high resolution TEM (HRTEM) image of the CNTs dispersed in the three-pass FSP composite. Fig. 5(a) indicates that CNTs were randomly and relatively uniformly dispersed in the Al matrix. Due to their random arrangement, the length of CNTs seemed to be much smaller than that identified in Fig. 4. Fig. 5(b) and (c) (d) shows that the tube structure of the CNTs was well retained, the CNT/Al interfaces were bonded well, and no voids were detected, which implied that good transfer load efficiency could be obtained. The formation of  $\text{Al}_4\text{C}_3$  has been described and discussed in our previous investigation [24].  $\text{Al}_4\text{C}_3$  was observed to form in the locations of CNT damage in four-pass FSP CNT/2009Al composites due to the reaction of Al and C atoms. However, the content of the  $\text{Al}_4\text{C}_3$  was very low and did not exert a significant effect on the strength of the composites [24].

In a previous work, Izadi et al. [21] showed that multi-walled CNTs (MWCNTs) were entirely destroyed after 3 passes of FSP. This is quite different from the present study. This difference is attributed to following two factors. Firstly, 4.5 vol.% CNTs were pre-distributed into the Al matrix by PM in the present study, while about 50 vol.% CNTs were simply pre-set into the groove machined on the plate in Ref. [21]. This implies that generally, indirect contact between CNTs and tool would occur during FSP in this study. Secondly, a much faster travel speed ( $\sim 100 \text{ mm/min}$ ) was used in this investigation.

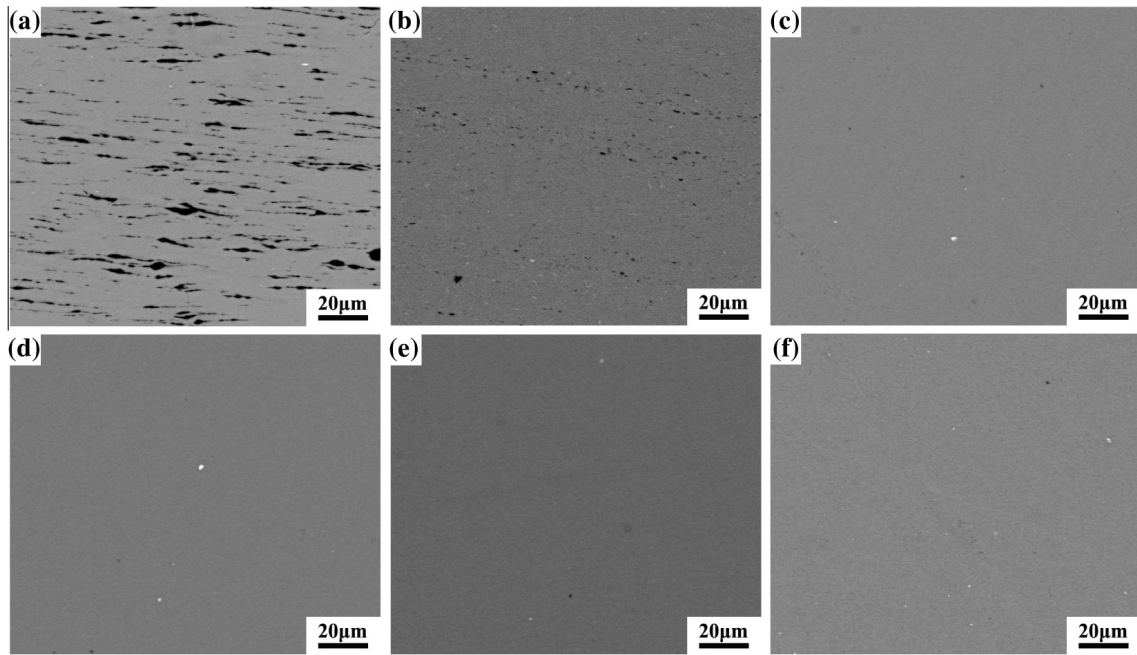


Fig. 3 – Backscatter SEM images showing CNT distribution in 4.5 vol.% CNT/2009Al composites: (a) forged, (b) one-pass FSP, (c) two-pass FSP, (d) three-pass FSP, (e) four-pass FSP, and (f) five-pass FSP.

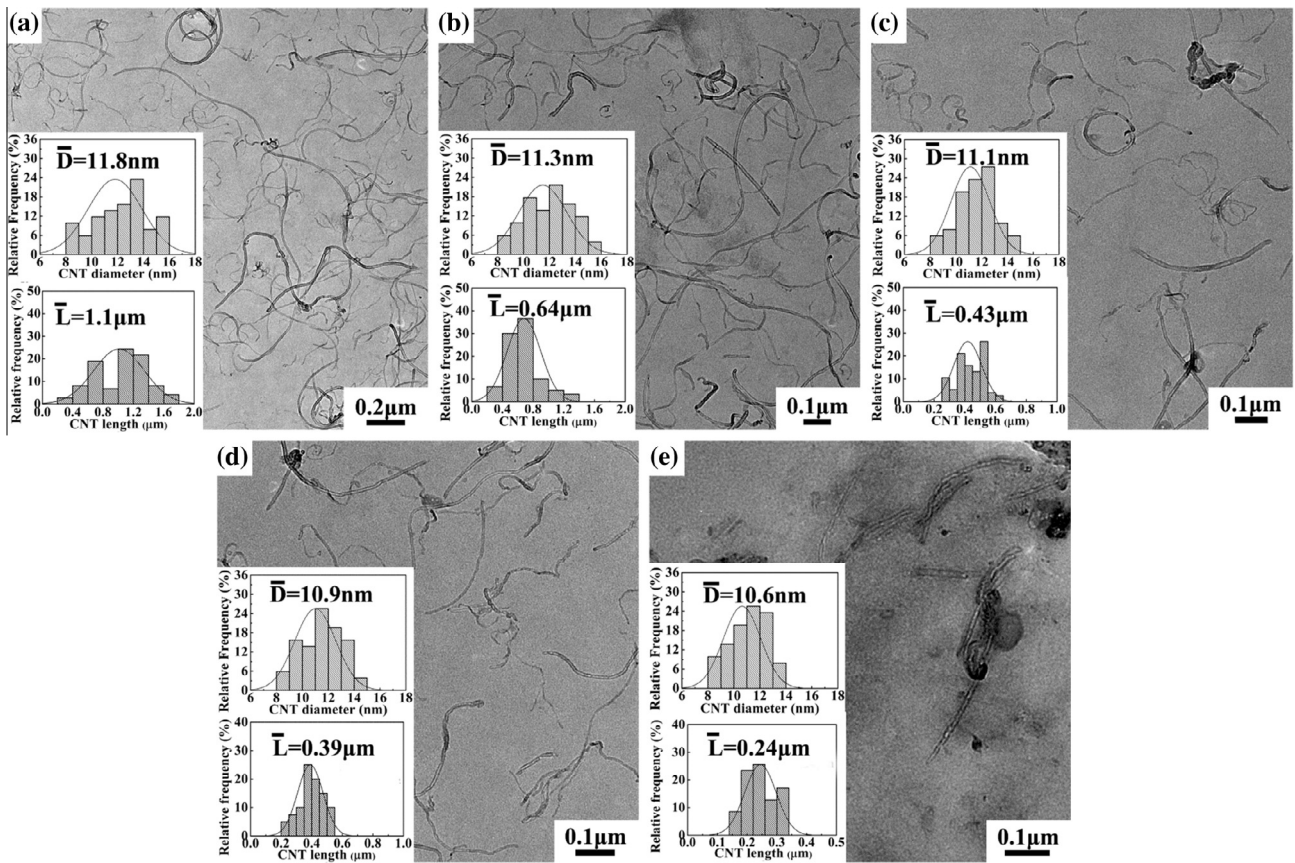
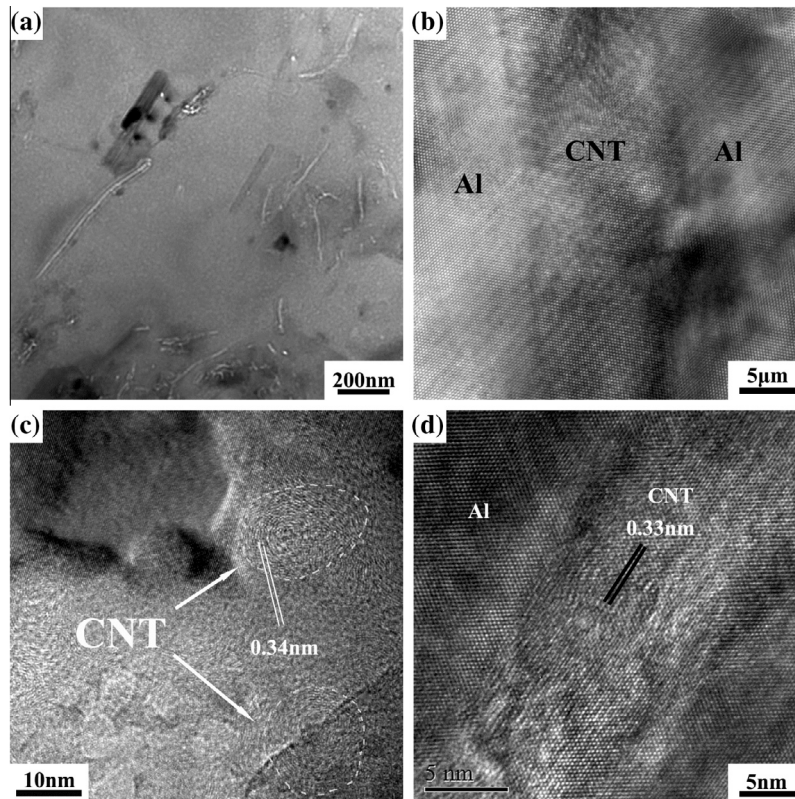


Fig. 4 – Morphologies and statistical lengths and diameters (inserts) of extracted CNTs at different numbers of FSP passes: (a) one pass, (b) two passes, (c) three passes, (d) four passes, and (e) five passes.



**Fig. 5 – (a) Dispersed CNTs, (b) HRTEM image of the CNT-Al interface, and (c) (d) tube structure of CNT in three-pass FSP 4.5 vol.% CNT/2009Al composite.**

This means that a much lower mechanical energy input was applied during FSP for this work. These two factors reduced the damage to the CNTs significantly, thereby retaining the tube structure.

Fig. 6 shows the grain structure of the forged and FSP composites. In the forged composite, the CNT clusters were distributed along grain boundaries, and the average grain sizes parallel and perpendicular to the forging direction were about 5 and 10  $\mu\text{m}$ , respectively. In the FSP composites, the average grain sizes were much finer. The one-pass FSP composite had a mean grain size of about 2–3  $\mu\text{m}$ . As the FSP pass increased, the grain size decreased gradually. After three-pass FSP a sub-micrometer grain size ( $\sim 800$  nm) was obtained.

It was documented that the grain sizes of aluminum alloys after plastic deformation were determined by the Zener–Holloman parameters [25]. In this case, similar FSP parameters should lead to similar grain sizes in the aluminum alloys. However, this study indicated that the grain size of the composites decreased as the number of FSP passes increased. This should be attributed to the effective pinning of CNTs on the grain boundaries. According to Zener’ theory [26], the pinning force is given by:

$$F = \frac{3}{2} \gamma \frac{f}{r} \quad (1)$$

where  $F$  is the pinning force,  $\gamma$  is the grain boundary energy,  $f$  is the volume fraction of the particle and  $r$  is the radius of the particle.

Firstly, the CNT clusters were significantly reduced and more CNTs were dispersed into the aluminum matrix as

the number of FSP passes increased, resulting in more uniform CNT distribution. Secondly, the CNTs were cut shorter by the FSP pass, producing a more effective pinning effect. This means that larger concentration and smaller size of the CNTs were achieved as the number of FSP passes increased, which led to increased pinning effect according to Eq. (1). Thus, unlike in the matrix alloy, the grain size in the composites decreased as the number of FSP passes increased.

### 3.2. Tensile properties

Table 1 shows the densities and tensile properties of the matrix alloys and composites under forging and different FSP conditions. The densities and tensile properties of the forged 2009Al alloy and FSP 2009Al alloys with different FSP passes were fundamentally identical, indicating that FSP did not improve the density and mechanical properties of the 2009Al alloy. However, for the 4.5 vol.% CNT/2009Al composites, the situation is quite different.

The forged composite had the lowest densities and tensile properties because the CNTs were mostly distributed as clusters. The CNT clusters without filling of aluminum matrix definitely caused the strength and ductility of the composite to deteriorate because the clusters could not bear the load and it was easy to induce stress concentration and micro-void nucleation. This could also be reflected in the tensile curve in Fig. 7 that the forged composite quickly fractured after elastic stage. The density and tensile properties of the FSP

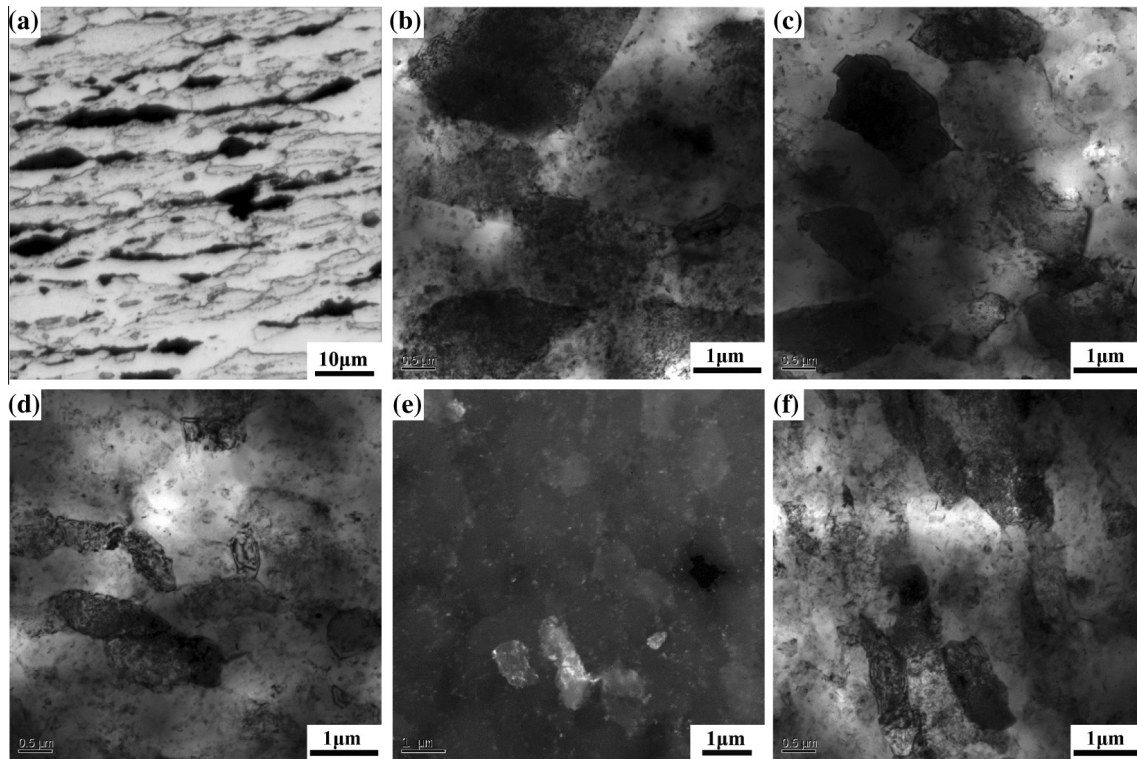


**Fig. 6 – Grain microstructure of 4.5 vol.% CNT/2009Al composites: (a) forged, (b) one-pass FSP, (c) two-pass FSP, (d) three-pass FSP, (e) four-pass FSP, and (f) five-pass FSP.**

**Table 1 – Densities and tensile properties of 2009Al and CNT/2009Al composites.**

Material		Density (g/cm <sup>3</sup> )	YS (MPa)	UTS (MPa)	El. (%)
2009Al alloy	Forged	2.757 ± 0.002	299 ± 7	411 ± 10	12 ± 2
	1-pass FSP	2.755 ± 0.002	297 ± 5	421 ± 8	13 ± 1
	3-pass FSP	2.754 ± 0.001	305 ± 3	416 ± 3	12 ± 2
	5-pass FSP	2.759 ± 0.001	305 ± 5	417 ± 4	15 ± 1
4.5 vol.% CNT/2009Al	Forged	2.642 ± 0.004	273 ± 10	298 ± 11	1 ± 0.5
	1-pass FSP	2.679 ± 0.003	406 ± 11	417 ± 9	2 ± 0.5
	2-pass FSP	2.695 ± 0.001	426 ± 8	437 ± 8	2 ± 1
	3-pass FSP	2.708 ± 0.001	451 ± 6	478 ± 8	3 ± 1
	4-pass FSP	2.704 ± 0.001	435 ± 8	466 ± 4	4 ± 1
	5-pass FSP	2.705 ± 0.002	420 ± 7	442 ± 5	4 ± 0.5

<sup>a</sup>Theoretical density of 2009Al ~2.750 g/cm<sup>3</sup> and that of MWCNTs is ~1.8 g/cm<sup>3</sup> [27].

<sup>b</sup>Theoretical density of 4.5 vol.% CNT/2009Al ~2.705 g/cm<sup>3</sup>.

composites were significantly enhanced due to reduced CNT clustering and improved CNT distribution compared to those of the forged composite and increased continuously as the number of FSP passes increased to three. The elongation change of the composites was obvious, as shown in Fig. 7. The composites exhibited the work-hardening as the number of FSP passes increased to 3 to 5, and as a result the ductility of the composite was increased.

It should be pointed out that the engineering stress–strain curves in Fig. 7 were obtained without using extensometer, thus the slopes of various stress–strain curves exhibit much lower values compared with the Young's modulus of aluminum (~70 GPa). However, it does not influence the determination of the strength of the composites.

The maximum strength was obtained with three-pass FSP due to the elimination of CNT clustering and more uniform CNT distribution. The YS of the three-pass FSP composite increased by about 64% compared to that of the forged composite. When the number of FSP passes increased further from three to five, the densities of the composites remained unchanged due to the similar CNT dispersion. However, both the YS and the ultimate tensile strength (UTS) of the five-pass FSP composite decreased due to reduced CNT length (this will be discussed in detail in the Section 4).

Three typical fractographs of 4.5 vol.% CNT/2009Al composites are shown in Fig. 8. For the forged composite (Fig. 8(a)), CNT clusters were frequently observed on the fracture surface. This is because that the CNT clusters resulted in

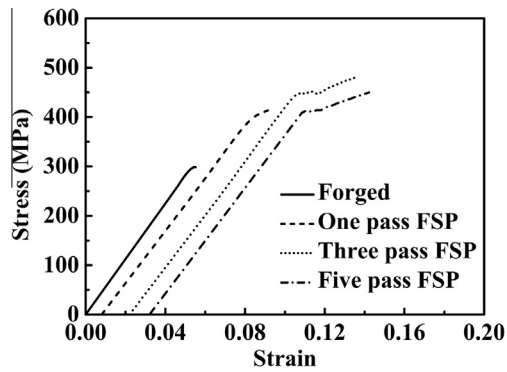


**Fig. 7 – Tensile curves of 4.5 vol.% CNT/2009Al composites with different FSP passes.**

stress concentration, inducing micro-void nucleation in the aluminum matrix nearby. For the one-pass FSP composite (Fig. 8(b)), both CNT clusters and dispersed CNTs could be found on the fracture surface, which was in accordance with the CNT distribution style in Fig. 3(b). When more than three FSP passes were applied, no CNT clustering was detected and the CNTs with a short pulled-out length were observed to be homogeneously distributed on the fracture surfaces (as shown by black arrows in Fig. 8(c)). This is consistent with the CNT distribution, as shown in Figs. 3(c) and 5(a).

Pulled-out CNTs with a short length have also been reported by other researchers. Jiang et al. [28] fabricated CNT/Al composites with uniformly dispersed CNTs. Although the CNTs had a length of about 0.5–2  $\mu\text{m}$ , only the CNTs with a short pulled-out length could be observed on the fracture surface. This has been attributed to two reasons. On one hand, the interface of the CNT tip and Al was subjected to large tensile stress during tension. The micro-pores tended to aggregate near the tips and to initiate cracks. On the other hand, the CNT tube–Al interface was strongly bonded. It was difficult for the cracks to propagate along the CNT interface, and

thus the CNTs on the fracture surfaces showed a short pulled-out length.

## 4. Discussion

### 4.1. CNT shortening

As shown in Fig. 4, the CNTs were shortened during FSP. Similarly, CNT shortening was also observed during other dispersing processes, such as ball-mill processing [19]. The length of CNTs affects the mechanical properties of CNT/metal composites greatly. Therefore, it is necessary to control the processes of dispersion and fabrication to reduce the CNT shortening. Furthermore, the CNTs were also artificially cut short by ball milling or shear mixing processing for special use in hydrogen storage [29,30] and molecular sieves [31]. The length of CNTs affects their physical properties greatly. In this case, it is important to predict the CNT length variation to optimize the fracture processes.

In this study, a model is proposed to describe CNT shortening and it is expected to provide guidance for CNT dispersion processing or CNT cut processing. The decrease in CNT length is mainly due to large plastic strains during processing. In order to describe the variation in the CNT length, let us assume that the fracture of CNTs occurs due to the flow of the matrix around the CNTs or the shear strain imposed on the CNTs and that the probability of CNT fracture is dependent on the CNT volume (for simplicity a linearized Weibull model [32] is used). With the above assumptions, the probability of fracture of a CNT  $p$  is:

$$p = kD^2L\varepsilon \quad (2)$$

where  $k$  is a constant that is related to CNT ultimate strain and could be considered as a constant for a given CNT,  $D$  is the CNT diameter,  $L$  is the CNT length, and  $\varepsilon$  is the imposed strain on a CNT during processing.

An assumption is made as follows: if a CNT with a length  $L$  fractures under an increment of strain  $d\varepsilon$ , it changes into two

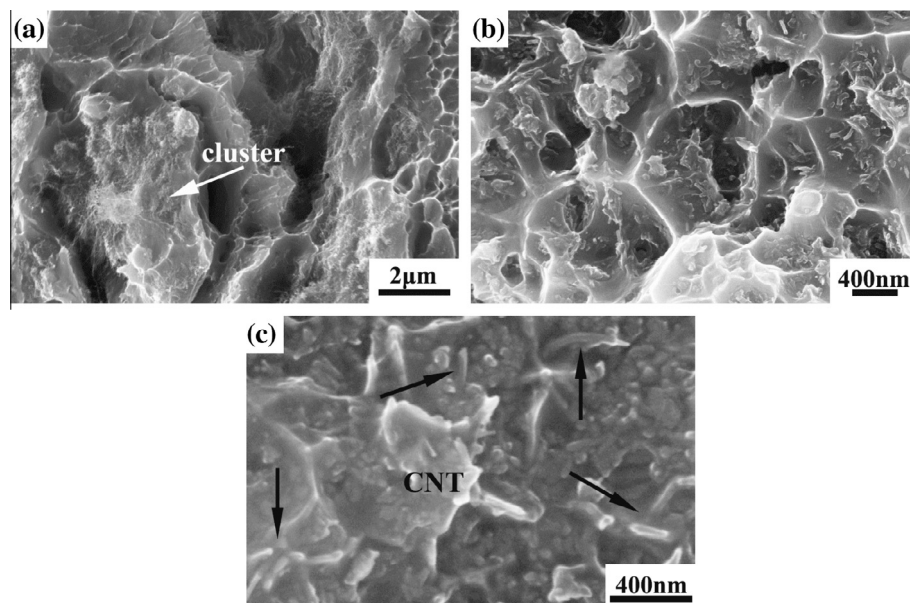


**Fig. 8 – Fractographs of 4.5 vol.% CNT/2009Al composites: (a) forged, (b) one-pass FSP, and (c) three-pass FSP.**

CNTs rather than three or more CNTs. This is acceptable because the strain increment of  $d\varepsilon$  is so small. As a result, the two resultant short CNTs have an average length of  $L/2$  (Fig. 9). Thus during an increment of strain  $d\varepsilon$  the change in the CNT length is  $KD^2Ld\varepsilon(L - L/2)$

That is,

$$\frac{dL}{d\varepsilon} = -kD^2L(L - L/2) \tag{3}$$

and hence, during a processing history with equivalent strain of  $\varepsilon$ , we can write:

$$\frac{1}{L} - \frac{1}{L_0} = \frac{1}{2}kD^2\varepsilon \tag{4}$$

where  $L_0$  is the CNT length before this processing and  $L$  is the CNT length after this processing.

If similar processing is repeated for  $n$  cycles, the CNT length can be expressed as:

$$\frac{1}{L_n} - \frac{1}{L_0} = \frac{n}{2}kD^2\varepsilon \tag{5}$$

where  $L_n$  is the length of CNTs after  $n$  cycles of similar processing. The CNT concentration is not considered as it was unchanged or varied little during the processing.

Multi-pass FSP could be considered as such a repeated processing, and Eq. (5) implies that the reciprocal of CNT length should exhibit a linear relationship with the FSP pass if the flow strain  $\varepsilon$  during different FSP passes is considered constant. Actually, the assumption of constant flow strain during different FSP passes is reasonable because the rotation rate and the travel speed were unchanged. Fig. 10 shows that the variation in the CNT length is in reasonable agreement with the prediction by Eq. (5); that is,  $L^{-1}$  has an approximately linear relationship with the FSP pass, with a correlation coefficient of 0.96.

In order to prove the wide suitability of Eq. (5), the experimental results of CNT shortening from previous investigations [33–37] were analyzed. Fig. 11 shows the variation of the CNT length with the duration of ball milling. Clearly, a linear relationship could be found for either single-walled CNTs (SWCNTs) or MWCNTs. Fig. 12 shows the relationship of the CNT length with the high speed shear count from [38]. The reciprocal of the CNT length increased linearly with the processing count. These analyses indicate that Eq. (5) could describe the CNT length evolution during CNT cut processing well.

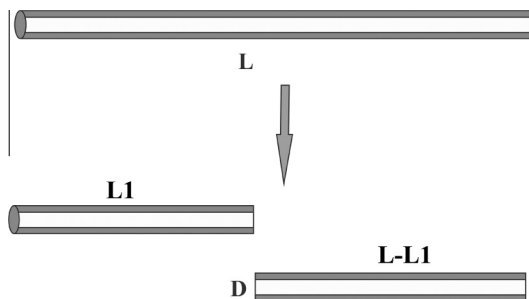


Fig. 9 – Schematic of CNT shortening model: CNT fractured into two short parts under an increment of strain  $d\varepsilon$ .

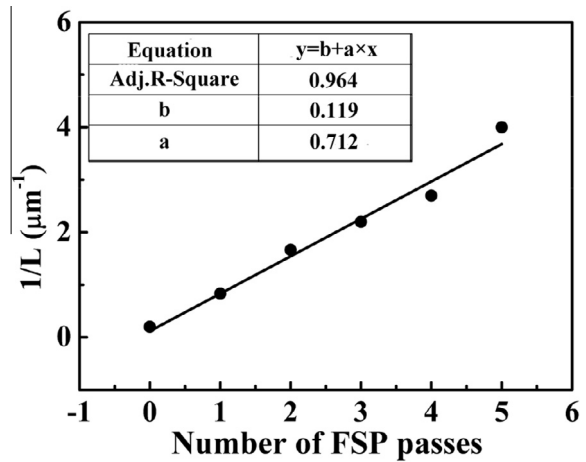


Fig. 10 – Variation of  $L^{-1}$  with the number of FSP passes. (Adj. R-Square is the correlation coefficient of the equation).

Based on the experimental data of the CNT length in the present study and the previous investigations, the CNT shortening during mechanical processing can be described well by Eq. (5). As a result of the different facilities and the different process parameters, the actual strain  $\varepsilon$  in the mechanical processing is complicated. Furthermore, it is difficult to obtain the parameter  $k$  due to different CNT fabrication routes and CNT sources. Fortunately, the CNT length variation can be predicted well if the original CNT length and the CNT length after some durations or passes of the processing are obtained. This provides a robust basis for predicting and controlling the CNT shortening during the CNT/Al composite fabrication and the mechanical cut processing of CNTs.

#### 4.2. Change in strength of composites

The variation in the tensile strength, relative density, grain size, and aspect ratio with increasing FSP passes can be explained by the following two reasons. Firstly, CNT clustering decreased with the number of FSP passes and thus the densities of the composites increased because CNT clustering resulted in the formation of pores in the composites, as shown in Fig. 3(a). Secondly, the CNTs were cut shorter and the grain size of the matrix gradually became finer. Thus the strengthening by CNT incorporation varied as the number of FSP passes increased.

Bakshi et al. [39] analyzed the strength results of the previous researchers and found that the load-transferring mechanism contributed to the strength increase if the CNTs were uniformly dispersed. Our previous investigation [24] proposed a strength equation based on the grain refinement and the load transfer. The YS of the CNT/Al composites with individually dispersed CNTs at room temperature could be expressed by:

$$\sigma_c = (\sigma_0 + kd^{-1/2})[V_f(s + 4)/4 + (1 - V_f)] \tag{6}$$

where  $\sigma_0$  is rationalized as a frictional stress, which could be simply considered as the strength of the alloy with coarse grains,  $d$  is the matrix grain size in the composite,  $k$  is the Hall-Petch slope and for Al-Cu-Mg alloy it is about

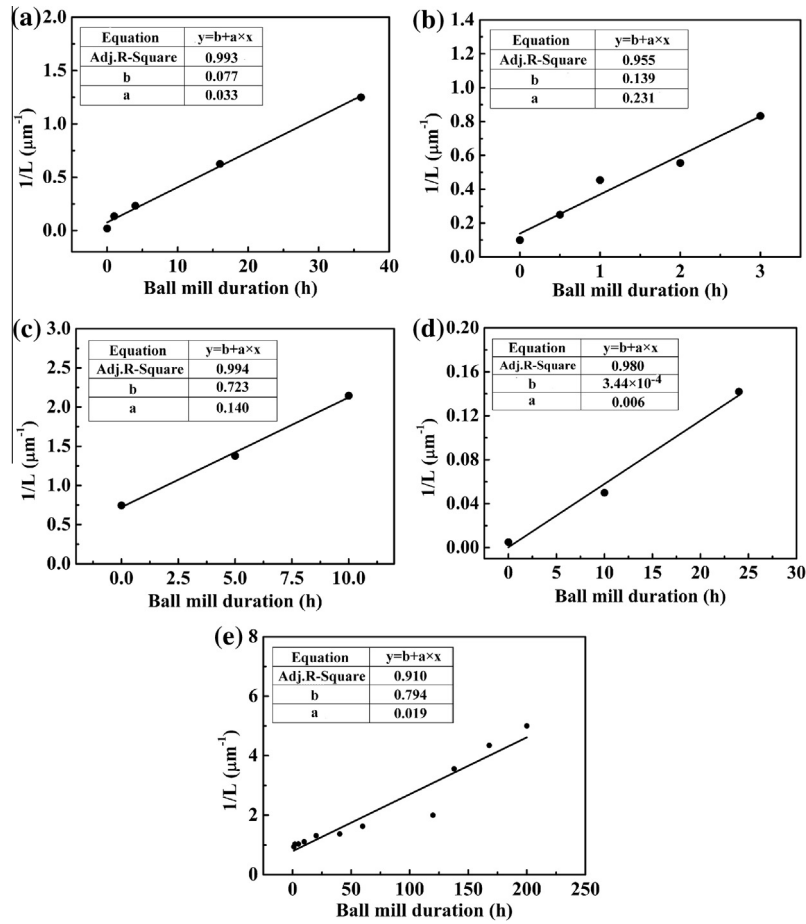


Fig. 11 – Variation of  $L^{-1}$  during CNT cutting with ball-milling duration for (a) MWCNTs from [33] and (b) SWCNTs from [34] (some data were discarded because the CNT length became longer as the duration of ball milling increased), (c) MWCNTs from [35], (d) MWCNTs from [36], and (e) MWCNTs from [37].

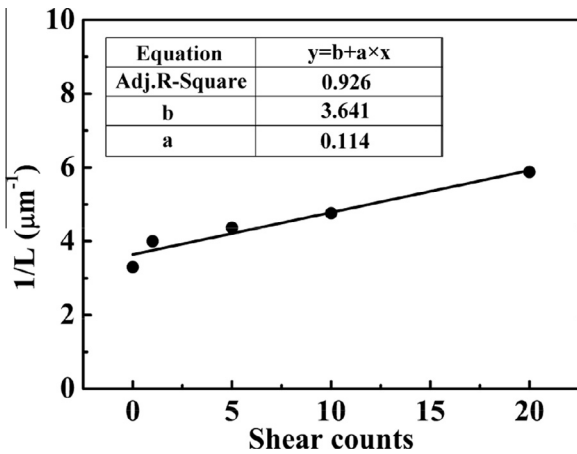


Fig. 12 – Variation of  $L^{-1}$  during CNT cutting with high speed shear count for MWCNTs from [38].

$0.1 \text{ MPa m}^{1/2}$  [24],  $\sigma_c$  is the YS of the composite,  $s$  is the aspect ratio of the CNTs, and  $V_f$  is the volume fraction of the CNTs.

Because of the existence of CNT clustering, the effective CNT volume fraction  $V_e$  that could actually transfer load is changed to:

$$V_e = V_f - V_{\text{cluster}} \tag{7}$$

where  $V_{\text{cluster}}$  is the volume fraction of CNT clusters.

Furthermore, the pores with irregular shapes led to high stress concentrations and the pores located at the CNT/Al interfaces reduced the bonded area at the interfaces, thereby decreasing the efficiency of load transfer from Al to CNTs. All of these factors could result in decreased strength of the composites. Several empirical expressions for the relationship between the strength and porosity of PM-processed materials have been proposed, assuming that the strength is a function of sintered density, as proposed by Squire [40]. The relationship between the strength and porosity is generally expressed as:

$$\sigma_L = \sigma_c \exp(-\lambda \theta) \tag{8}$$

where  $\sigma_L$  is the strength of composite with pores,  $\theta$  is the volume fraction of porosity, and  $\lambda$  is a constant for material with porosity. For 2009Al alloy,  $\lambda$  is about 15.5 [41,42].

The volume fraction of porosity can be estimated by density measurement as follows:

$$\theta = 1 - \frac{\rho}{\rho_{\text{Al}}(1 - V_f) + \rho_{\text{CNT}}V_f} \tag{9}$$

where  $\rho$  is the measured density of the composite,  $\rho_{\text{Al}}$  is the theoretical density of the matrix alloy, and  $\rho_{\text{CNT}}$  is the

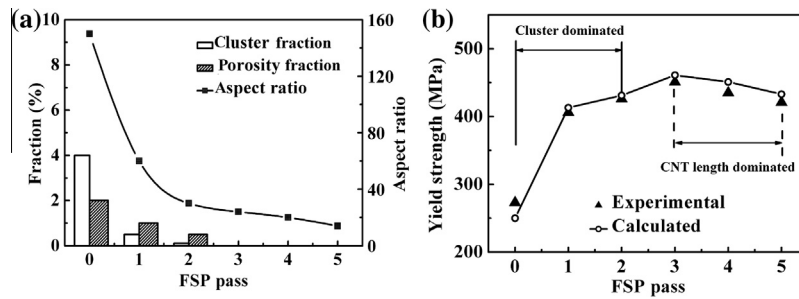


**Fig. 13 – (a) Variation of clustering and porosity fractions as well as aspect ratio with number of FSP passes; (b) comparison of experimental and calculated YS.**

theoretical density of the CNTs and is  $\sim 1.8 \text{ g/cm}^3$  [27]. After FSP, the CNT density could be deemed to be changed little because the CNTs were tube shape and the diameters were well retained, although the CNTs were cut shorter. Thus, the theoretical density of  $\sim 1.8 \text{ g/cm}^3$  for CNTs was still used in Eq. (9) for calculation.

Combining the effects of the above microstructural parameters, that is, the aspect ratio of CNTs and the grain size and porosity volume fraction of the composites, an equation is proposed to estimate the tensile strength of CNT/2009Al composites:

$$\sigma_L = (\sigma_0 + kd^{-1/2})[(V_f - V_{\text{cluster}})(s + 4)/4 + (1 - (V_f - V_{\text{cluster}}))\exp(-\lambda\theta)] \quad (10)$$

As the number of FSP passes increased, the volume fraction of the clusters and pores and the aspect ratio of CNTs in the multi-pass FSP composites decreased, as shown in Fig. 13(a). The YS values calculated by Eq. (10) using the parameters in Fig. 13(a) are shown in Fig. 13(b). The calculated values of YS are in good agreement with the experimental results. For the composites with zero to two FSP passes, weak load transfer efficiency and stress concentration due to the CNT clusters led to the lower strength of the CNT/Al composites. As the number of FSP passes increased to more than three, the shorter CNTs reduced the strengthening effect of the CNTs significantly. Thus, as a compromise, the maximum strength was obtained with three-pass FSP.

It should be pointed out that the concentration of CNT clusters used in Eq. (10) was a little overestimated, because not all black zones in Fig. 3 were CNT clusters. Porosity might exist around or inside the clusters. As a result, the predicted strength of the composites with clustering should be a little underestimated. However, the calculated strengths are in good agreement with the experimental results. This implies that this model somewhat overestimates the strength of the composites with clustering. This means that the constant  $\lambda$  in Eq. (10) for the CNT/2009Al composites was a little smaller than that for the 2009Al alloy.  $\lambda$  is known to be related to the shape and size of pores [42]. The smaller value of  $\lambda$  indicates that the strength is less sensitive to the pores for the CNT/2009Al composites. It is believed that the pores within the CNT clusters in the CNT/2009Al composites would lead to less stress concentration. Thus a smaller value of  $\lambda$  was induced compared with that in the 2009Al alloy. Clearly, for the CNT/Al composites both with individually dispersed CNTs and

with CNT clusters and pores, the strengths of the composites could be predicted by Eq. (10).

## 5. Conclusions

4.5 vol.% CNT/2009Al were fabricated by a combination of PM and FSP. As the number of FSP passes increased, the CNT clustering fraction decreased and the CNTs were dispersed into the aluminum matrix. The homogeneously distributed CNTs resulted in a finer grain size of the matrix. The mechanical strengths of the CNT/2009Al composites were improved significantly after FSP and the maximum strength increase was obtained with three-pass FSP.

The CNTs were cut short after FSP due to the shear effect. The CNT length decreased as the number of FSP passes increased. A CNT shortening model is proposed to describe the evolution of CNT length during mechanical processing. The model predicts that the reciprocal of CNT length has a linear relationship with the number of processing cycles, which is in good agreement with the experimental results for FSP of CNT/metal composites and the CNT shortening in ball-mill or processing involving fracture or shear-cutting.

A universal strength model is proposed to describe the strengthening of the CNT/Al composites with or without the CNT clusters, based on the grain size of the matrix, the aspect ratio of the CNTs, and the volume fraction of the CNT clusters and pores. The model predictions are in good agreement with the experimental results.

## Acknowledgments

The authors gratefully acknowledge the support of (a) the National Basic Research Program of China under grant Nos. 2011CB932603 and 2012CB619600 and (b) the National Natural Science Foundation of China under grant No. 51331008.

## REFERENCES

- [1] Krishnan A, Dujardin E, Ebbesen TW, Yianilos PN, Treacy MMJ. Young's modulus of single-walled nanotubes. *Phys Rev B* 1998;58(20):14013–9.
- [2] Wong EW, Sheehan PE, Lieber CM. Nanobeam mechanics: elasticity, strength, and toughness of nanorods and nanotubes. *Science* 1997;277(5334):1971–5.

- [3] Salvétat-Delmotte J-P, Rubio A. Mechanical properties of carbon nanotubes: a fiber digest for beginners. *Carbon* 2002;40(10):1729–34.
- [4] Poncharal P, Wang ZL, Ugarte D, De WA. Electrostatic deflections and electromechanical resonances of carbon nanotubes. *Science* 1999;283(5407):1513–6.
- [5] Qian D, Wagner GJ, Liu WK, Yu M-F, Ruoff RS. Mechanics of carbon nanotubes. *Appl Mech Rev* 2002;55(6):495–533.
- [6] Curtin WA, Sheldon BW. CNT-reinforced ceramics and metals. *Mater Today* 2004;7(11):44–9.
- [7] Kim YA, Hayashi T, Endo M, Gotoh Y, Wada N, Seiyama J. Fabrication of aligned carbon nanotube-filled rubber composite. *Scripta Mater* 2006;54(1):31–5.
- [8] Ahmad I, Unwin M, Cao H, Zhu YQ. Multi-walled carbon nanotubes reinforced Al<sub>2</sub>O<sub>3</sub> nanocomposites: mechanical properties and interfacial investigations. *Compos Sci Technol* 2010;70(8):1199–206.
- [9] Kuzumaki T, Miyazawa K, Ichinose H, Ito K. Processing of carbon nanotube reinforced aluminum composite. *J Mater Res* 1998;13(9):2445–9.
- [10] Zhou SM, Zhang XB, Ding ZP, Min CY, Xu GL, Zhu WM. Fabrication and tribological properties of carbon nanotubes reinforced Al composites prepared by pressureless infiltration technique. *Compos A* 2007;38(2):301–6.
- [11] Bakshi SR, Lahiri D, Agarwal A. Carbon nanotube reinforced metal matrix composites – a review. *Int Mater Rev* 2010;55:41–64.
- [12] Bakshi SR, Keshri AK, Agarwal A. A comparison of mechanical and wear properties of plasma sprayed carbon nanotube reinforced aluminum composites at nano and macro scale. *Mater Sci Eng, A* 2011;528(9):3375–84.
- [13] Nam DH, Cha SI, Lim BK, Park HM, Han DS, Hong SH. Synergistic strengthening by load transfer mechanism and grain refinement of CNT/Al–Cu composites. *Carbon* 2012;50(7):2417–23.
- [14] Kwon H, Estili M, Takagi K, Miyazaki T, Kawasaki A. Combination of hot extrusion and spark plasma sintering for producing carbon nanotube reinforced aluminum matrix composites. *Carbon* 2009;47(3):570–7.
- [15] Stein J, Lenczowski B, Frety N, Anglaret E. Mechanical reinforcement of a high-performance aluminium alloy AA5083 with homogeneously dispersed multi-walled carbon nanotubes. *Carbon* 2012;50(6):2264–72.
- [16] Wang L, Choi H, Myoung JM, Lee W. Mechanical alloying of multi-walled carbon nanotubes and aluminium powders for the preparation of carbon/metal composites. *Carbon* 2009;47(15):3427–33.
- [17] Suryanarayana C. Mechanical alloying and milling. *Prog Mater Sci* 2001;46(1–2):1–184.
- [18] Esawi AMK, El Borady MA. Carbon nanotube-reinforced aluminium strips. *Compos Sci Technol* 2008;68(2):486–92.
- [19] Esawi AMK, Morsi K, Sayed A, Taher M, Lanka S. Effect of carbon nanotube (CNT) content on the mechanical properties of CNT-reinforced aluminium composites. *Compos Sci Technol* 2010;70(16):2237–41.
- [20] Kwon H, Park DH, Silvain JF, Kawasaki A. Investigation of carbon nanotube reinforced aluminum matrix composite materials. *Compos Sci Technol* 2010;70(3):546–50.
- [21] Izadi H, Gerlich P. Distribution and stability of carbon nanotubes during multi-pass friction stir processing of carbon nanotube/aluminum composites. *Carbon* 2012;50(12):4744–9.
- [22] Johannes LB, Yowell LL, Sosa E, Arepalli S, Mishra RS. Survivability of single-walled carbon nanotubes during friction stir processing. *Nanotechnology* 2006;17(12):3081–4.
- [23] Morisada Y, Fujii H, Nagaoka T, Fukusumi M. MWCNTs/AZ31 surface composites fabricated by friction stir processing. *Mater Sci Eng, A* 2006;419(1–2):344–8.
- [24] Liu ZY, Xiao BL, Wang WG, Ma ZY. Singly dispersed carbon nanotube/aluminum composites fabricated by powder metallurgy combined with friction stir processing. *Carbon* 2012;50(5):1843–52.
- [25] Humphreys FJ, Hatherly M. Recrystallization and related annealing phenomena. 2nd ed. UK: Elsevier Ltd; 2004. p. 427.
- [26] Maazi N, Rouag N. Consideration of Zener drag effect by introducing a limiting radius for neighbourhood in grain growth simulation. *J Cryst Growth* 2002;243(2):361–9.
- [27] Ma PC, Siddiqui NA, Marom G, Kim JK. Dispersion and functionalization of carbon nanotubes for polymer-based nanocomposites: a review. *Composites A* 2010;41(10):1345–67.
- [28] Jiang L, Li ZQ, Fan GL, Cao LL, Zhang D. The use of flake powder metallurgy to produce carbon nanotube (CNT)/aluminum composites with a homogenous CNT distribution. *Carbon* 2012;50(5):1993–8.
- [29] Dillon C, Jones KM, Bekkedahl TA, Bethune DS, Heben MJ. Storage of hydrogen in single-walled carbon nanotubes. *Nature* 1997;386:377–9.
- [30] Dresselhaus MS, Williams KA, Eklund PC. Hydrogen in carbon materials. *MRS Bull* 1999;24(11):45–9.
- [31] Wang Q, Challo SR, Sholl DS, Johnson JK. Quantum sieving in carbon nanotubes and zeolites. *Phys Rev Lett* 1999;82(5):956–9.
- [32] Weibull W. A statistical distribution function of wide application. *J Appl Mech* 1951;18:293–7.
- [33] Pierard N, Fonseca A, Konya Z, Willems I, Van Tendeloo G, Nagy JB. Production of short carbon nanotubes with open tips by ball milling. *Chem Phys Lett* 2001;335(1–2):1–8.
- [34] Pierard N, Fonseca A, Colomer JF, Bossuot C, Benoit JM, Van Tendeloo G, et al. Ball milling effect on the structure of single-wall carbon nanotubes. *Carbon* 2004;42(8–9):1691–7.
- [35] Kukovec A, Kanyo T, Konya Z, Kiricsi I. Long-time low-impact ball milling of multi-wall carbon nanotubes. *Carbon* 2005;43:994–1000.
- [36] Kim YA, Hayashi T, Fukai Y, Endo M, Yanagisawa T, Dresselhaus MS. Effect of ball milling on morphology of cup-stacked carbon nanotubes. *Chem Phys Lett* 2002;355:279–84.
- [37] Krause B, Villmow T, Boldt R, Mende M, Petzold G, Potschke P. Influence of dry grinding in a ball mill on the length of multiwalled carbon nanotubes and their dispersion and percolation behaviour in melt mixed polycarbonate composites. *Compos Sci Technol* 2011;71:1145–53.
- [38] Jang BK, Sakka Y. Dispersion and shortening of multi-walled carbon nanotubes by size modification. *Mater Trans Jpn Inst Met* 2010;51(1):192–5.
- [39] Bakshi SR, Agarwal A. An analysis of the factors affecting strengthening in carbon nanotube reinforced aluminum composites. *Carbon* 2011;49(2):533–44.
- [40] Lenel FV. Powder metallurgy principles and application. Princeton: Metal Powder Institute Federation; 1980. p. 233–4.
- [41] Liu ZY, Wang QZ, Xiao BL, Ma ZY. Clustering model on the tensile strength of PM processed SiCp/Al composites. *Compos A* 2010;41(11):1686–92.
- [42] Hong SH, Chung KH. Effects of vacuum hot pressing parameters on the tensile properties and microstructure of SiC-2124Al composites. *Mater Sci Eng, A* 1995;194(2):165–70.